Electrochemical solid–solid conversion of bismuth oxide to bismuth metal

Oliver Pyper, Brigitte Hahn and Robert Schöllhorn

Institut für Anorganische und Analytische Chemie, Technische Universität Berlin, Strasse des 17. Juli 135, D-10623 Berlin, Germany

It is shown that binary and ternary bismuth oxides can be reduced quantitatively in aqueous electrolytes at ambient temperature *via* a two-phase solid–solid transition by electron/proton transfer to metastable porous metal and alloy systems. Single-crystal studies demonstrate the pseudomorphous character of the transition; topochemical correlations between educt and product phase could not be established, however. The solid-state reaction may proceed even at rather low temperatures of $-40\,^{\circ}C$.

In a recent publication a concept has been discussed that concerns the controlled formation of metastable porous homogeneous and heterogeneous systems by the electrochemical reduction of transition-metal oxides, chalcogenides and halides to the corresponding metal systems *via* electron/proton transfer at ambient temperature in a solid–solid conversion.[1] The basic validity of the reaction scheme has been demonstrated with copper compounds as the example. Prerequisites for this type of reaction are a low enthalpy of formation of the metal compound and a thermodynamically or kinetically accessible redox potential of the metal cation–metal couple. Many oxides of the p-block main-group metals are known to exhibit moderate enthalpies of formation, *e.g.* the oxides of the heavier elements thallium, lead and bismuth. We have performed a study on the reactivity of bismuth(III) oxide, which has been proposed in earlier investigations as electrode material in primary batteries with aprotic electrolytes.[2–4] We report here on the solid–solid conversion of Bi_2O_3 in aqueous electrolytes and on similar reactions of some related binary bismuth compounds. Since the potential formation of new metastable alloys is a principal aspect in our investigations of these solid–solid reactions we also included studies on appropriate ternary bismuth phases.

Experimental

Bismuth oxide, Bi_2O_3, was prepared by sintering pressed pellets (diameter 12 mm, thickness *ca.* 1 mm) of the carbonate $(BiO)_2CO_3$ for 20 h at 750 °C. Ternary bismuth phases with Cu, Pb, W, Yb were obtained by sintering of the binary oxides in the appropriate stoichiometric ratio according to the literature: Bi_2CuO_4,[5] $Pb_2Bi_6O_{11}$,[6] $(Bi_2O_3)_{0.75}(WO_3)_{0.25}$,[7] $Bi_{1.714}Yb_{0.286}O_3$.[8,9] The oxyhalides BiOCl,[10] BiOI[11] and the oxyacetate $BiO(CH_3CO_2)$[12] were prepared by crystallization from aqueous solutions. Large natural single crystals were used in the case of bismuth sulfide, Bi_2S_3.

Electrochemical reactions were performed in three-electrode cells with commercial potentiostat equipment, a Hg/HgO reference electrode and 0.1 mol dm^{-3} KOH as the standard electrolyte. Working electrodes were sintered pellets, contacted by platinum clamps, or, in the case of oxyhalides and bismuth oxyacetate, in platinum grid-pressed powder electrodes with 1 mass% PTFE. Bismuth sulfide crystals were contacted by platinum clamps.

For structural investigations by powder X-ray diffractometry the Guinier technique and a powder diffractometer (Siemens D5000, linear counter) were used with Cu-Kα radiation. Further characterization was achieved by transmission electron microscopy (JEOL JSEM 200 B) and scanning electron microscopy with an EDX analytical probe (Hitachi S-2700/Kevex). Magnetic susceptibility data were obtained using a Faraday balance.

Results and Discussion

Reduction of bismuth oxide

Preliminary investigations on the cathodic reduction of sintered Bi_2O_3 pellets in aqueous neutral electrolyte showed the formation of a metallic grey zone around the platinum contact site which spread rapidly across the entire pellet surface; the end point of the reduction was indicated by the sudden formation of hydrogen gas. Analytical investigations confirmed the quantitative conversion of the oxide to bismuth metal according to eqn. (1).

$$Bi_2O_3 + 6H^+ + 6e^- \rightarrow 2Bi^0 + 3H_2O \quad (1)$$

The potential *vs.* charge transfer diagram for the galvanostatic cathodic reduction of Bi_2O_3 working electrodes in 0.1 mol dm^{-3} aqueous KOH in air atmosphere is given in Fig. 1. The initial strong overpotential is due to the small original reaction zone at the platinum point contact. Bi_2O_3 is a wide bandgap semiconductor and the reaction can start only at the small metallic lead (Pt)/Bi_2O_3/electrolyte triphase boundary. Further progress of the reaction occurs subsequently at the bismuth metal/Bi_2O_3 moving boundary zone. Since the Bi_2O_3/Bi interface area increases rapidly in the initial reaction period the overvoltage decreases strongly and is followed by a potential plateau. Towards the end of the reaction the interface region diminishes again which results in an increasing overpotential. The end of the solid–solid conversion is indicated by a potential step and the formation of molecular hydrogen at the working electrode. If the reduction is carried out in contact with air the experimental charge transfer observed (as determined by the potential step) is usually somewhat higher compared to the calculated value of 6 e^- per Bi_2O_3. Under an inert gas atmosphere (nitrogen, argon) charge-transfer data

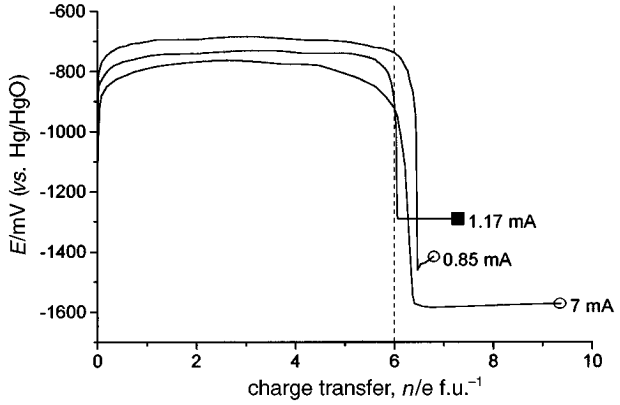

Fig. 1 Potential *vs.* charge transfer diagram for the cathodic reduction of Bi_2O_3 working electrodes in 0.1 mol dm^{-3} KOH at different current values (300 K); ○, air; ■, N_2 atmosphere

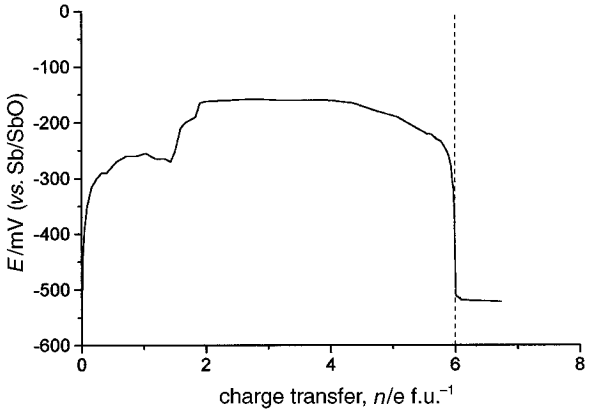

Fig. 3 Low-temperature galvanostatic reduction of Bi_2O_3 at $T = -40\,^{\circ}C$; (electrolyte 7 mol dm^{-3} aqueous KOH; sintered pellet working electrode, mass 392 mg, current 5 mA)

close to the theoretical value are found owing to the absence of oxygen. The influence of the current density is illustrated in Fig. 2. In contact with air low current densities (*i.e.* long reaction times) lead to strongly increased values for the charge transfer due to the partial oxidation of Bi at the cathode by O_2. High current densities result in a strong overpotential leading to slow discharge of hydrogen as a competing process. No significant influence of the variation of the electrolyte concentration (0.1–10 mol dm^{-3}) and of the electrolyte cation (Li, Na, K) on the charge transfer could be observed.

We were interested to find out whether this solid-state reaction would proceed also at temperatures below 25 °C with reasonable kinetics. The experiment was carried out in a cryostat at −40 °C with concentrated aqueous KOH (7 mol dm^{-3}) as the electrolyte in order to avoid solidification. The galvanostatic curve is given in Fig. 3. The initial region is characterized by a strong overpotential followed by a potential plateau. The sharp potential step indicates a charge transfer of 6 e^- f.u.$^{-1}$ (f.u. = formula unit) in very good agreement with the calculated value. It is surprising that this non-topotactic solid-state reaction can proceed with reasonable reaction rates and quantitative conversion at rather low temperatures.

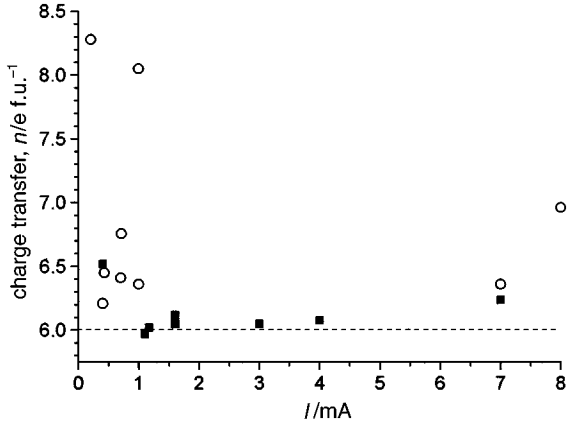

Fig. 2 Cathodic reduction of Bi_2O_3 in aqueous KOH: dependence of the nominal charge-transfer values upon the cell current; ○, air; ■, N_2 atmosphere

The potential plateau observed in the galvanostatic reduction of Bi_2O_3 to Bi suggests a two-phase process, in agreement with the reaction assumed by eqn. (1). This is confirmed by the X-ray diffraction data given in Fig. 4, which confirm the coexistence of the oxide educt Bi_2O_3 and the metal product Bi; no intermediate phase can be detected.

In order to determine the reduction potential in potentiostatic mode a step-screening experiment was performed (potential step chronocoulometry). At a potential of −750 mV *vs.* the Hg/HgO reference electrode, a charge transfer of 5.9 e^- f.u.$^{-1}$ could be measured. The current *vs.* time diagram is given

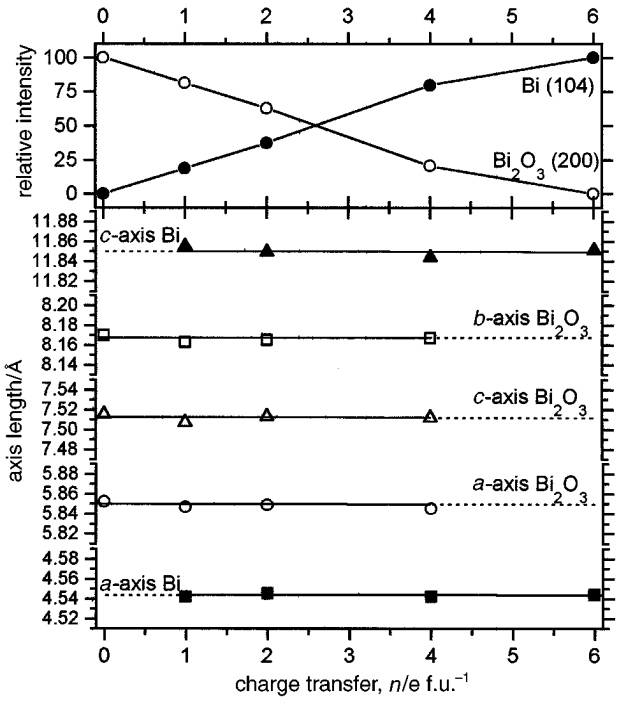

Fig. 4 Galvanostatic reduction of Bi_2O_3. Upper section: change of relative intensities of selected educt and product reflections with the charge transfer; lower section: observed lattice parameters of the coexisting phases *vs.* charge transfer.

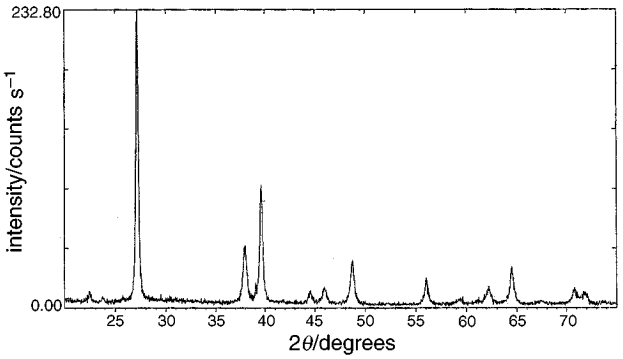

Fig. 6 X-Ray diffractogram of bismuth metal obtained by cathodic reduction of Bi_2O_3 at $-40\,^{\circ}C$ (*cf.* data given in Fig. 3)

in Fig. 5. The shape of the curve can be explained by the Bi_2O_3/Bi interface area change as discussed above; irregularities are assumed to be due to crack regions in the sintered sample. The quantitative charge transfer at a defined potential suggests again the conclusion that no potential intermediate phases appear.

The product obtained by cathodic reduction is brittle and exhibits a metallic grey colour. After washing in water and acetone and drying in vacuum the electrode mass was identical to the calculated value within $<1\%$; *i.e.* no residual electrolyte or water was retained in the pore system. The lattice parameters of the products prepared at $20\,^{\circ}C$ and $-40\,^{\circ}C$ were close to those reported in the literature. For samples prepared at ambient temperature the increase in Bragg linewidth was rather small as compared to well ordered polycrystalline bismuth metal. From particle size calculations[13] it can be assumed that the primary particles have a nominal diameter >500 Å. The linewidth broading increases with increasing diffraction angle, which suggests specific lattice defects. Bismuth metal prepared from Bi_2O_3 at $-40\,^{\circ}C$ showed, as expected, rather broad reflections, however, indicating strong lattice disorder (Fig. 6). A calculation of the nominal particle size (domains with coherent diffraction) yielded a value of <400 Å. SEM images showed crack regions at the surface (10 μm range); the resolution limit of the instrument used did not allow detection of the pore structure. Magnetic properties of the reduced samples were determined by dc susceptibility measurements in the temperature range 200–300 K; in agreement with literature data, diamagnetism was observed.

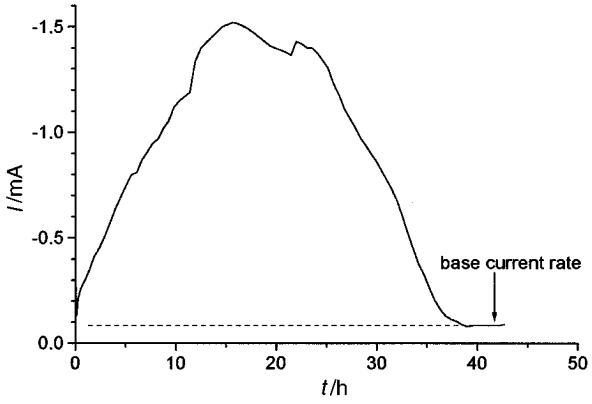

Fig. 5 Potential step chronocoulometry of a Bi_2O_3 electrode: current *vs.* time diagram for the reaction at -750 mV (0.1 mol dm^{-3} aqueous KOH, pressed sintered pellets of mass 100 mg). Area $= -37.2$ mA h

Reduction of single-crystal material

For a demonstration of the pseudomorphous character of the solid-state transformation under investigation and for the control of potential structural correlations between educt and product, single-crystal material is required. Bi_2O_3 crystals were not available but single crystals of bismuth oxychloride, BiOCl, and of bismuth sulfide, Bi_2S_3, could be obtained. We were able to show that both phases can be reduced quantitatively to bismuth metal according to

$$BiOCl + H_2O + 3e^- \rightarrow Bi^0 + 2OH^- + Cl^- \quad (2)$$

$$Bi_2S_3 + 3H_2O + 6e^- \rightarrow 2Bi^0 + 3OH^- + 3SH^- \quad (3)$$

BiOCl single crystals were obtained as platelets with quadratic shape. The crystals were rather small (edge length 5–10 μm) and very thin, which turned out to be most favourable for TEM investigations. Fig. 7 shows a TEM image, Fig. 8 an electron diffraction image of the single crystal used. The electrochemical reduction was performed in aqueous suspension in platinum vessels. TEM images after reduction confirmed that the morphology of the platelets was retained. Dark-field images displayed a system of interconnected metal clusters with an average particle diameter of 500–1000 Å. Electron diffraction studies showed that all lines of the pattern obtained could be attributed to crystalline bismuth metal (Fig. 9). There was no indication, however, for a preferential orientation of the metal particles identified.

In the case of the sulfide, Bi_2S_3, large metallic grey crystal

Fig. 7 TEM image of two BiOCl crystals. Dimensions of the smaller crystal *ca.* 5×5 μm.

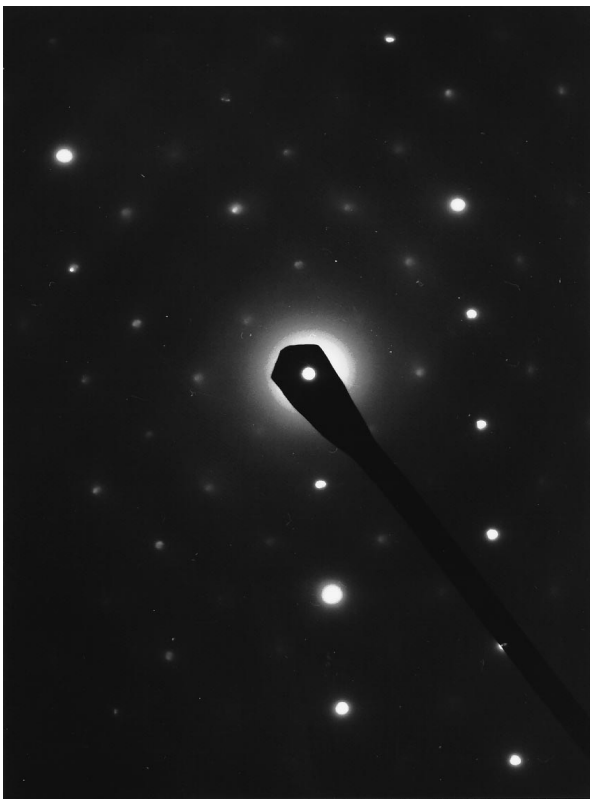

Fig. 8 Electron diffraction pattern of the BiOCl crystals shown in Fig. 7

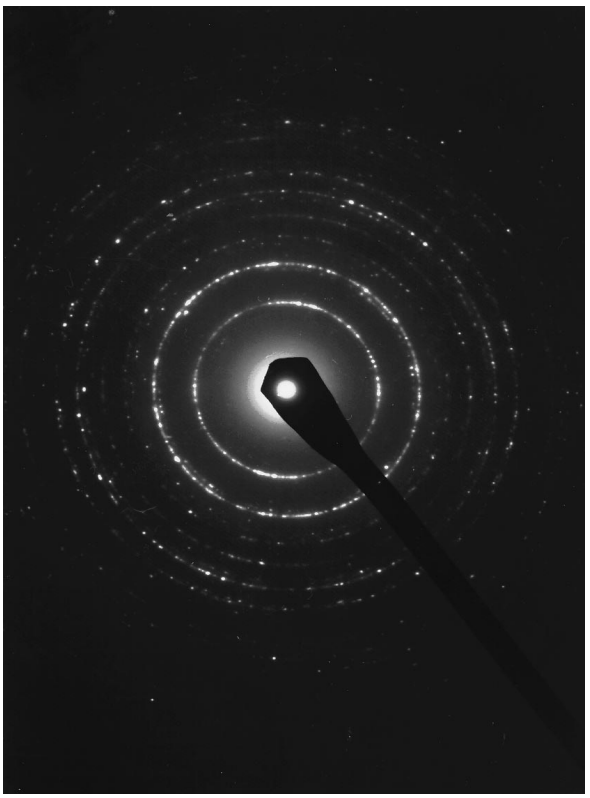

Fig. 9 Electron diffraction pattern of bismuth metal obtained by cathodic reduction of BiOCl. Beam diameter *ca.* 0.5 μm.

agglomerates from a natural source (bismuthinite, Namibia, Helikon II, East) were available. It was possible to isolate needles with $0.3 \times 0.3 \times 0.8$ mm^3 size by cleaving. Galvanostatic reduction yielded a charge transfer equivalent to 5.9 e^- f.u.$^{-1}$; X-ray data confirmed that the product was bismuth metal. EDX–SEM studies demonstrated that, independent of the location of the current lead contact point, the reaction started synchronously at all crystal edges and at local crystal defects, which is a consequence of the high conductivity of the narrow bandgap semiconductor sulfide. X-Ray rotation photographs of Bi_2S_3 crystal needles (*c* axis perpendicular to X-ray beam, observation of 0*k*0 reflections) were made before and after reduction. In the latter case only faintly structured closed diffraction cone cross-sections could be observed. It must be concluded again that there is no correlation between the initial orientation of the Bi_2S_3 crystal and the orientation of the metal crystallites present after reduction, although the transition is clearly pseudomorphous.

Reduction of ternary bismuth oxides

The principal idea here was to prove the possibility of the preparation of a metastable porous alloy and heterogeneous phases *via* low-temperature electrochemical conversion of appropriate oxide systems;[1] an overview is given in Table 1.

Bismuth and copper are not miscible in the solid state,[14] the reduction of bismuth oxocuprate, Bi_2CuO_4, at 300 K could therefore be expected to lead to the formation of a metastable amorphous alloy since the related binary oxides Bi_2O_3 and CuO can both be reduced to metal. The potential *vs.* charge transfer curve for the reduction of sintered Bi_2CuO_4 working electrodes in 0.1 mol dm^{-3} KOH under an inert gas atmosphere is given in Fig. 10. The electrochemical charge-transfer value of 8.2 e^- f.u.$^{-1}$ correspond reasonably well with the value calculated according to eqn. (4).

$$Bi_2CuO_4 + 4H_2O + 8e^- \rightarrow (Bi_2/Cu) + 8(OH)^- \qquad (4)$$

The X-ray diagram of the product exhibits a strong background with broadened reflections corresponding to bismuth metal while no other lines, in particular no reflections that can be attributed to copper metal, can be detected. This may be understood in terms of a mixture of an amorphous metastable copper–bismuth alloy along with a fraction of crystalline bismuth metal. An alternative interpretation of the X-ray data could be based, however, on a model that involves microdomains of copper metal, too small to give appreciable diffraction intensity, in a bismuth matrix. EXAFS measurements are in progress to decide between the two models. If this material is heated to 650 °C for 12 h in closed evacuated quartz ampoules then X-ray data reveal the presence of the diffraction lines of bismuth as well as of copper metal (along with some weak reflections belonging to Bi_2O_3, indicating surface oxidation of the product). Similar results have been obtained in our earlier investigations on the electrochemical reduction of superconducting $Bi_2Sr_2CaCu_2O_{8+x}$.[15]

Yellow–orange sintered pellets of the ternary bismuth–lead oxide $Pb_2Bi_6O_{11}$ could be reduced electrochemically to a grey product with a metallic appearance; the charge transfer value of 21.9 e^- f.u.$^{-1}$ found experimentally is in agreement with the

Table 1 List of bismuth compounds investigated

material	prep.[a]	symmetry	$n_{calc.}$[b]	$n_{obs.}$[b]	E_D[c]/mV
Bi_2O_3	$(BiO)_2CO_3$ (750 °C)	monoclinic	6	6.2 (20 °C) 6.0 (−40 °C)	−755
Bi_2S_3	mineral (xx)	orthorhombic	6	5.9	−1050
BiOCl	ref. 10 (xx)	tetragonal	3	3.15	−750
BiOI	ref. 11	tetragonal	3	3.15	−660
BiO(ac)[d]	ref. 12	tetragonal	3	3.15	−720
Bi_2CuO_4	ref. 5	tetragonal	6 (Bi)+2 (Pb)	8.2	−750
$Pb_2Bi_6O_{11}$	ref. 6	monoclinic	4 (Pb)+18 (Bi)	21.9	−750/−1050
$Bi_{14}W_2O_{27}$	ref. 7, 18	tetragonal	42 (Bi)	43	−1100
$Bi_{1.72}Yb_{0.28}O_3$	ref. 9	cubic	5.14 (Bi)	5.3	−720

[a]xx = Single crystal. [b]n = Charge transfer (e^- f.u.$^{-1}$). [c]E_D = Potential for reduction *vs.* Hg/HgO reference electrode measured under current. [d]ac = CH_3CO_2.

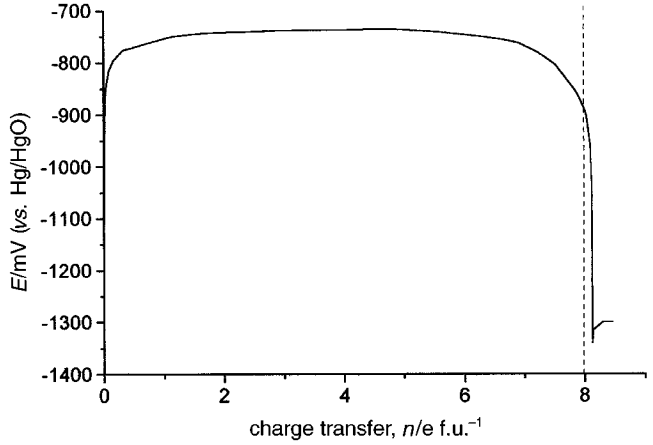

Fig. 10 Potential *vs.* charge transfer diagram for the cathodic reduction of Bi_2CuO_4 (sintered pellet contacted with platinium clamp, mass 650 mg, current 3 mA, 0.1 mol dm^{-3} aqueous KOH as electrolyte, N_2 atmosphere)

calculated value of 22 e^- if both lead and bismuth are reduced to the metallic state [eqn (5)].

$$Pb_2Bi_6O_{11} + 22H_2O + 22e^- \rightarrow (Pb_2/Bi_6) + 22OH^- \quad (5)$$

Upon exposure to air the grey material changes to grey–black over a few hours owing to oxidation processes.

The Pb/Bi phase diagram exhibits only one intermediate ε-phase around the composition Pb_7Bi_3.[16] X-Ray diagrams of the reduction product indicate the presence of bismuth metal and Pb_7Bi_3[17] as the major crystalline components (along with traces of Pb_3O_4, probably due to oxidation). Only two weak lines corresponding to Pb metal could be detected. After exposure of reduced samples to air for 3 weeks at 300 K continued oxidation takes place: besides the reflection of bismuth metal and Bi_2O_3 a series of lines corresponding to α-PbO were found, while the lines associated with Pb_7Bi_3 and Pb had virtually disappeared. We conclude that the freshly reduced product does contain also a component of amorphous lead–bismuth alloy.

For studies on the preparation of heterogeneous metal–non-reducible oxide porous systems the two ternary phases $(Bi_2O_3)_{0.75}(WO_3)_{0.25}$ (described as cubic)[7] and $Bi_{1.72}Yb_{0.28}O_3$[8,9] (cubic) were selected (Table 1). We assumed that in both cases only Bi^{3+} could be reduced to the metal while tungsten and ytterbium oxide should remain as dispersed phases in the metal matrix.

X-Ray investigations of sintered pellets of the yellow–green bismuth–tungsten oxide found mainly single-phase $Bi_{14}W_2O_{27}$ (tetragonal).[18] They could be reduced galvanostatically with a charge-transfer value of 43 e^- f.u.$^{-1}$ as compared with the calculated value of 42 e^- f.u.$^{-1}$ based on eqn. 6.

$$Bi_{14}W_2O_{27} + 42H_2O + 42e^- \rightarrow 14Bi + 2WO_3 + 42OH^- \quad (6)$$

The X-ray diffractogram of the product exhibit only the lines for bismuth metal except for a few additional reflections that could not be indexed reliably owing to the low line intensities. Obviously tungsten oxide remains as an amorphous oxide–hydrate fraction in the product.

$Bi_{1.72}Yb_{0.28}O_3$ can be considered as a rare-earth-metal stabilized δ-Bi_2O_3. The X-ray diagram of the reduction product shows the lines for bismuth metal along with a strong background in the lower 2θ range. Amorphous ytterbium oxide–hydroxide is assumed to be dispersed in the metal matrix.

An attempt was made to reduce a bismuth compound with rather large anions (*i.e.* a strong spatial 'dilution' of Bi^{3+}) in order to find out whether the line width and particle size of the product would increase and decrease respectively. The compound selected was bismuth oxyacetate; the X-ray data of the reduction product did not however exhibit line broadening superior to that found for the cathodic reduction of bismuth oxide.

Reoxidation reactions

Samples prepared by reduction of Bi_2O_3 undergo slow visible oxidation upon storage in air at 300 K: after several days changes from metallic grey to golden yellow and blue–black could be observed while no measurable change in mass or X-ray diffraction pattern was detected. Upon electrochemical oxidation of bismuth metal (prepared from Bi_2O_3) similar changes in colour are observed. If samples are first oxidized until the potential of O_2 gas formation is reached and subsequently reduced, then a charge transfer of *ca.* 0.3 e^- f.u.$^{-1}$ at −740 mV can be measured. Quantitative reoxidation is thus not possible; the high stability of thin oxide layers on bulk bismuth metal upon electrochemical oxidation has been described earlier.[19]

Conclusions

The processes investigated belong to an interesting specific type of low-temperature solid-state reaction. The exact mor-

phology of the microscopic pore structure has not been established so far, it may depend on several parameters.[1] The data of the present study on bismuth compounds favour the model of a matrix system built up from approximately isometric metal cluster units rather than a sponge-like structure similar to, *e.g.*, reticulated glassy carbon materials. The results of a preliminary scanning tunnelling electron microscopy study on the reduction of a copper oxide single crystal also appear to support the cluster model;[20] it seems problematic, however, to conclude from structures found in the surface region on the architecture of the bulk material. X-Ray diffraction, electron diffraction and TEM studies do not exhibit texture effects, *i.e.* there seems to be no measurable correlation between the starting lattice and the product phase.

We acknowledge the support of the work by the DFG Deutsche Forschungsgemeinschaft, Bonn, Germany.

References

1 G. Pfletschinger, B. Hahn and R. Schöllhorn, *Solid State Ionics*, 1996, **84**, 151.
2 J. O. Besenhard and H. P. Fritz, *Electrochim. Acta*, 1975, **20**, 513.
3 P. Fiordiponti, G. Pistoia and C. Temperoni, *J. Electrochem. Soc.*, 1978, **125**, 14.
4 G. Pistoia, *J. Power Sources*, 1985, **16**, 263.
5 K. Sreedhar and P. Ganguly, *Inorg. Chem.*, 1988, **27**, 2261.
6 JCPDS, International Centre for Diffraction Data, Newtown Square, PA, 1990, PDF card no. 41-0404.
7 Y. J. Lee, C. O. Park, H. D. Baek and J. S. Hwang, *Solid State Ionics*, 1995, **76**, 1.
8 H. Iwahara, T. Esaka, T. Sato and T. Takahashi, *J. Solid State Chem.*, 1981, **39**, 173.
9 JCPDS, International Centre For Diffraction Data, Newtown Square, PA, 1990, PDF card no. 41-0288.
10 G. Brauer, *Handbuch der präparativen anorganischen Chemie*, Ferdinand Enke Verlag, Stuttgart, 1975, p. 596.
11 Gmelin, *Handbuch der anorganischen Chemie*, vol. 19 (Wismut), VCH, Weinheim, 1964, pp. 722ff.
12 B. Aurivillius, *Acta Chem. Scand.*, 1955, **9**, 1213.
13 H. P. Klug and L. E. Alexander, *X-ray diffraction procedures*, Wiley, New York, 1974, 2nd edn., p. 695.
14 M. Hansen, *Constitution of binary alloys*, McGraw-Hill, New York, 1958, p. 308.
15 R. Bezzenberger, E. Gocke and R. Schöllhorn, *Fiz. Nizk. Temp.* (*Kharkov*), 1990, **16**, 572.
16 M. Hansen, *Constitution of binary alloys*, McGraw-Hill, New York, 1958, p. 325.
17 S. Rasmussen and B. Lundtoft, *Powder Diffraction*, 1987, **2**, 28; PDF card no. 39-1087.
18 A. Watanabe, N. Ishizawa and M. Kato, *J. Solid State Chem.*, 1985, **60**, 252; PDF card no. 39-0061.
19 Gmelin, *Handbuch der anorganischen Chemie*, vol. 19 (Wismut), Verlag Chemie, Berlin, 1927, pp. 23, 81.
20 G. Krüger, N. Breuer and R. Schöllhorn, unpublished work.
21 JCPDS, International Centre for Diffraction Data, Newtown Square, PA, 1992, PDF card no. 44-1246.

Paper 6/05939B; *Received* 28*th August*, 1996